# Evaluation of gravity dependence of lunar surface bearing capacity

## Evaluation de l'impact gravitationnel lunaire sur la portance

T. Kobayashi, K. Omine, Y. Suyama
*Faculty of Engineering, Kyushu University, Japan*
R. Ishikura
*Department of Civil Engineering, Yamaguchi University, Japan*

ABSTRACT

As a basic study for future lunar/planetary exploration missions, a series of model tests of shallow footing systems on a simulated lunar soil were conducted in partial gravity fields. Moreover, to rationally explain the dependence of ultimate bearing capacity on gravity, theoretical evaluations were attempted in the framework of the upper bound method. The proposed calculation method not only makes it possible to quantitatively correlate the failure mode with dependence on gravity, but also may allow us to predict the ultimate bearing capacity in the lunar surface environment.

RÉSUMÉ

Pour une étude de base concernant de futures missions lunaire/planétaire, une série de modèle a fondation superficielle sur une simulation de sollunaire a etait mener dans un champ a gravit partielle. De plus pour expliquer rationnellement l'impact gravitationnel sur laportance maximale, des évaluations théoriques ont tentative avec le cadre de la plasticit (borne supérieure). La méthode de calcul propos non seulement rend possible de quantitativement correspondre le mode d'échec avec l'impact de la gravit, mais aussi peut nous permettre de prédire laportance maximale a la surface de la lune.

Keywords : lunar surface, bearing capacity, upper bound method

## 1 INTRODUCTION

In January, 2004, National Aeronautics and Space Administration (NASA) announced a new vision for human and robotic space exploration, and declared that they send astronauts to the Moon until 2025. In September, 2007, the first Japanese lunar orbiter named "KAGUYA" was successfully launched by Japan Aerospace Exploration Agency (JAXA). The following month, China also launched an um-manned lunar orbiter "Chang'e -1". As seen in these trends of space missions, lunar and planetary exploration programs have been taking shape in several countries.

The future lunar exploration will involve various soil-related operations, including excavations, mining and foundation works for extraterrestrial facilities. Successful operations will rely on an understanding of the soil-machine and/or soil-structure interaction problems. In short, geotechnical evaluations of lunar surface are of fundamental importance in evaluating the feasibility of the missions.

Besides differences in the surface material, the lunar surface is subject to harsh environmental conditions such as low gravity, high vacuum, extreme temperatures and radiation. It is well known that the gravity on the Moon is approximately one-sixth that of Earth's gravity. In view of the fact that the self weight of soil significantly affects soil deformation and collapse, prediction of soil behaviors in a low gravity environment is of overriding importance. This paper attempts to examine the effects of gravity on load-settlement characteristics of shallow foundation systems, and to theoretically evaluate the dependence of the ultimate bearing capacity on gravity.

## 2 LUNAER REGOLITH AND LUNAR SOIL SIMULANT

Soils that cover the lunar/planetary surface are called "regolith". It has been reported that dust and very fine particles, having a few tens of micrometers in size, pulverized by meteorite impacts had accumulated and the stratum reaches to a depth of 20 to 30 meters at its deepest. Carrier et al. (1973 a) presented some photographs of real lunar soil, and mentioned that many (in some cases, most) of the particles are not compact, but exhibit irregular shapes and surface textures. This is because that abrasion by particle movements with wind or water does not occur on lunar surface. Form investigations of the lunar soil samples brought back by the Apollo (USA) and Luna (USSR) missions, it is known that lunar soil exhibits comparatively high particle density (approximately 3.0 g/cm$^3$) and has maximum and minimum bulk density of 1.82 g/cm$^3$ and 1.15 g/cm$^3$, respectively in average. Moreover, it is reported that relative density of the lunar surface is 74 $\pm$ 3 % in a depth range of 0 - 30 cm, and the stratum exhibits dense state of $D_r$ = 92$\pm$ 3 % when it comes to a depth of 30 - 60 cm (Carrier at el. 1993 b).

To make progress on researches and developments for diverse lunar missions, lunar soil simulants, which are made of terrestrial-based soils that mimic real regolith, are often used due to limited availability of real regolith. In Japan, JAXA had developed several simulants. In this study, a Japanese lunar soil

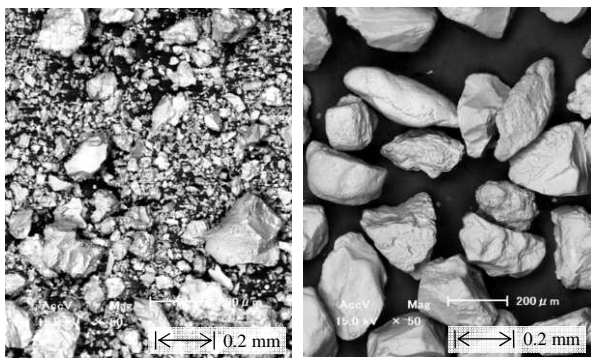


(a) Lunar soil simulant (b) Toyoura sand

Figure 1. SEM photographs of the materials.



*doi:10.3233/978-1-60750-031-5-656*

Table 1. Properties of the materials.

| Soil properties | Lunar soil simulant | Toyoura sand |
|---|---|---|
| Maximum bulk density, $\rho_{max}$ (g/cm³) | 2.02 | 1.64 |
| Minimum bulk density, $\rho_{mim}$ (g/cm³) | 1.49 | 1.34 |
| Maximum void ratio, $e_{max}$ | 0.98 | 0.98 |
| Minimum void ratio, $e_{min}$ | 0.46 | 0.62 |
| Particle density, $\rho_s$ (g/cm³) | 2.95 | 2.65 |
| Effective grain size, $D_{10}$ (mm) | 0.014 | 0.21 |
| Mean grain size, $D_{50}$ (mm) | 0.10 | 0.26 |
| Cohesion ($D_r$ = 60%), $c'$(kN/m²) | 1.44 | 3.04 |
| Cohesion ($D_r$ = 90%), $c'$(kN/m²) | 7.52 | 3.04 |
| Friction angle, ($D_r$ = 60%), $\phi'$(deg) | 41.6 | 38.1 |
| Friction angle, ($D_r$ = 90%), $\phi'$(deg) | 50.1 | 42.7 |

stimulant named FJS-1 (Kanamori et al. 1998) and Toyoura sand were used for the experiments. Targeted properties of the material include chemical composition, particle density, particle size distribution, and shear strength of the lunar samples brought back by the Apollo missions. The major raw material is basaltic lava rock mined from the Mt. Fuji area, and Ilmenite and Olivine were added for simulating the chemical composition of the actual lunar soil. The Scanning Electron Microscope (SEM) photographs and physical properties of the materials used are shown in Figure 1 and Table 1, respectively.

## 3 MODEL LOADING TESTS IN LOW GRAVITY FIELD

The bearing capacity problems relate to various situations in the surface operations, such as a touchdown of a landing module, supporting of a structure and machine, or even the walking of an astronaut. In this paper, to examine the effects of gravity on the load-settlement characteristics of shallow foundation systems, a series of model loading tests were conducted under low gravity conditions. The loading tests were performed on an aircraft that flew in parabolic paths to generate partial gravity fields. The aircraft starts to accelerate in a concave path, and then the thrust is suspended when the aircraft attains enough speed, after which partial gravity is kept for approximately 20 to 40 seconds in a convex path. Six variations of gravity were targeted in the tests, namely 0 g, 1/6 g, 1/2 g, 3/4 g, 1 g and 2 g. The gravity level of 2 g was achieved via the circular flight pattern.

A series of loading tests were performed with a footing installation system (Figure 2). The soil box is constructed of 10 mm-thick acrylic boards, and the upper end of the soil box is covered with an aluminum clamp so as to prevent the boards from bending. The size of the model ground is 400 mm in width, 160 mm in height and 50 mm in depth. In order to reduce the effects of friction between the soils and the boards, 0.02 mm thick latex membranes were laid between them, and silicon grease was applied between the boards and the membranes. The model grounds were prepared to have the relative densities of 60 % and 90 % for each soil, representing the bulk densities of 1.77 g/cm$^3$ and 1.95 g/cm$^3$ for the lunar soil simulant, and those of 1.51 g/cm$^3$ and 1.61 g/cm$^3$ for Toyoura sand. The model footing is made of aluminum and the size of the base is 20 mm in width and 50 mm in length. A piece of sandpaper was attached to the base so that the model would have a rough footing. The footing was designed to penetrate the model ground surface at a constant rate of 3.0 mm/s.

## 4 TEST RESULTS

The amount of settlement with respect to an arbitrary allowable bearing capacity is usually estimated based on a parameter called the coefficient of subgrade reaction, $K_s$, which is defined

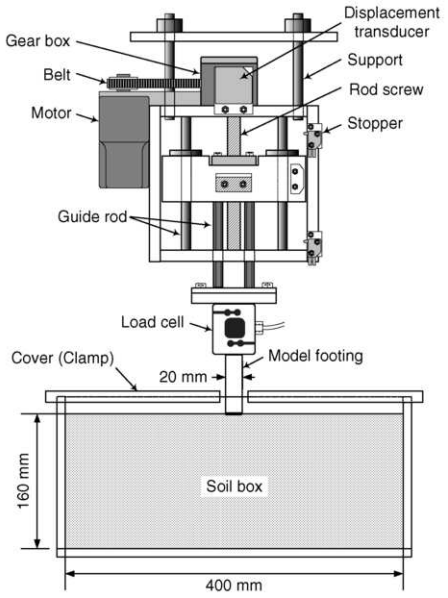


Figure 2. Model test apparatus.

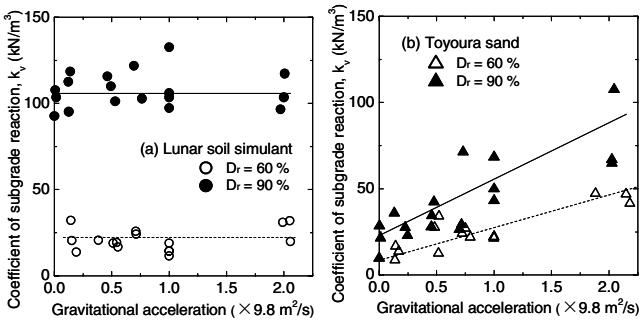


Figure 3. Effects of gravity on subgrade reaction.

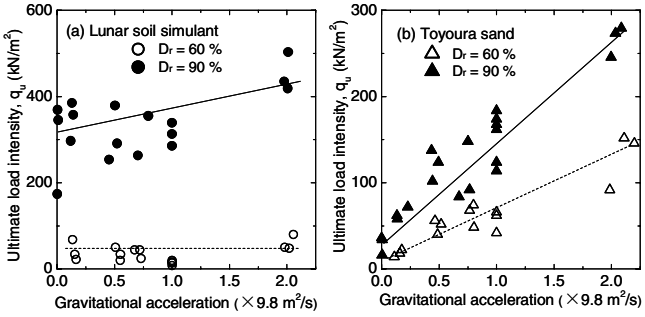


Figure 4. Effects of gravity on ultimate load intensity.

by a linear slope of the load-settlement curve. Figure 3 shows the effects of gravity on the coefficient of subgrade reaction, $K_s$. It is clear from this figure that gravity hardly influences $K_s$ for the lunar soil simulant (Figure 3(a)), whereas $K_s$ for Toyoura sand varies proportionally with the gravity levels (Figure 3(b)).

Figure 4 shows the effects of gravity on ultimate load intensity, $q_u$. This figure indicates that the $q_u$ values of Toyoura sand are in proportion to the gravity levels, regardless of how it is packed, whereas no clear proportionality between the gravity levels and the $q_u$ values can be found in the case of the lunar soil simulant partly due to the dispersion of the data. As to the case of $D_r$ = 60 % for the lunar soil simulant, gravity hardly influences the $q_u$. As to $D_r$ = 90 %, even if linearity on the relationships is assumed, the slope (sensitivity of gravity toward $q_u$) is still low compared to that of Toyoura sand. As discussed later in more details, in classical bearing capacity theories, the ultimate bearing capacity is in proportion to gravity. It is

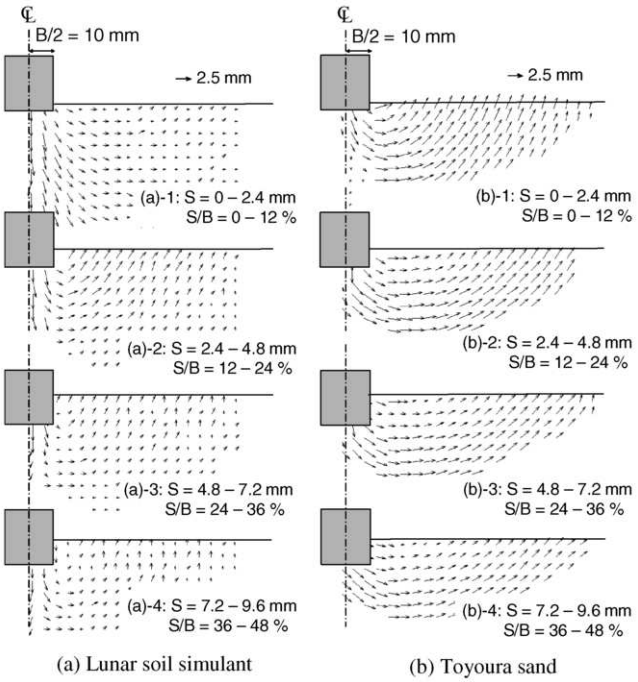


Figure 5. Displacement vectors of the soils ($D_r$ = 90 %, 1 g condition).

interesting that, while Toyoura sand exhibits such a proportional trend, it does not hold true for the lunar soil stimulant.

The differences in soil behavior are examined through observation of the soil. Figure 5 illustrates the displacement vectors of each materials of $D_r$ = 90 % under 1 g condition as the typical deformation mechanism. The displacement vectors of the soil particles were traced at intervals of 2.4 mm of settlement (S/B = 12 %) between 0 and 9.6 mm (S/B = 0 - 48 %) by using the Particle Image Velocimetry (PIV) technique.

The uppermost charts in the figure, which represent the vectors just after the installations, show that a general shear failure mode was seen in Toyoura sand (Figure 5(b)), while the lunar soil simulant formed a compression region below the footing (Figure 5(a)), followed by a deformation field that indicates a general shear failure. That is, the lunar soil simulant exhibits a phased failure mode where a local failure is first caused due to compression and is followed by a general shear failure. In the advanced stages of the footing installation, however, downward vectors can be seen and the compression still continues in the lunar soil simulant, while all soil particles under the footing moves sideways in the case of Toyoura sand. Moreover, through an examination of the process after the peak load in the lunar soil simulant, it was found that the magnitude of the vectors moving sideways in the lunar soil simulant is relatively smaller than that of Toyoura sand, indicating that the general shear failure mode seen in the lunar soil simulant is not as perfect as that in Toyoura sand.

## 5 EVALUATION OF GRAVITY DEPENDENCE

In general shear failure mode as seen in case of Toyoura sand, the passive failure zone spreads upward until the failure surface extends through the ground surface, causing the surface to swell as described in Figure 6(a). At that moment, the zone moving upward is doing work against gravity, and this appears to be the major factor in determining the dependence of the ultimate bearing capacity on gravity. In the case of the local shear failure mode as described in Figure 6(b), downward displacements are predominant and, thus, there is no work against gravity. In Figure 5(a), although the outward and/or upward soil displacements can be seen in the lunar soil simulant, the magnitude of such displacements is small compared to that in

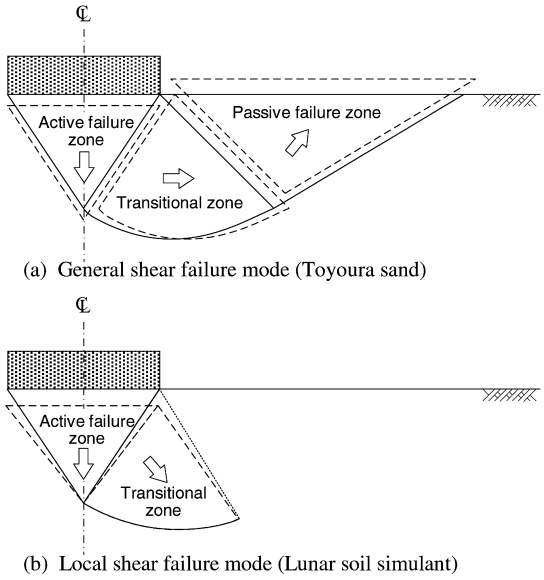


Figure 6. Schematics of observed failure mode.

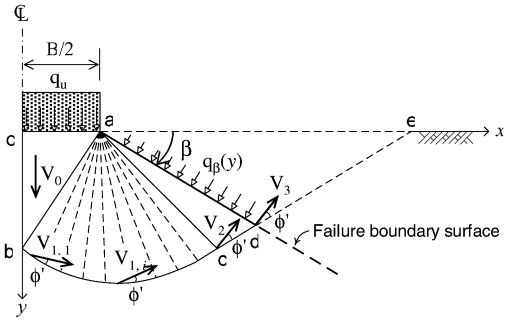


Figure 7. Assumed failure mechanism.

Toyoura sand, demonstrating that the effect of gravity was not present as prominently.

To quantitatively examine the relationship between gravity dependence and the failure mechanism, the upper bound method was applied in this paper. When a footing base is completely rough, the Plandtl mechanism is to be formed below the footing. In this paper, by incorporating a straight line, called "the failure boundary surface," which makes an angle of $\beta$ from the ground surface as shown in Figure 7, and by assuming that no deformation occurs on the outside of the failure boundary surface, we attempt to explain the punching or local shear failure mechanism in relation to soil compressibility. This is based on the notion that the failure region can be controlled by changing the value of $\beta$ according to the soil compressibility.

In the upper bound method, an equation related to the collapse load is built by calculating the total internal energy dissipation rate and the total external work rate in the assumed failure mechanism, and by equating the sum of these values. Furthermore, the solutions are obtained by changing the geometrical parameters, including $\beta$, that determine the failure region to minimize the collapse load.

## 6 CALCULATION RESULTS AND DISCUSSIONS

With the dimensional analysis, the ultimate bearing capacity can be non-dimensionalized by cohesion, $c$, and can be expressed as the functions of non-dimensionalized parameters as follows:

$$\frac{q_0}{c} = \frac{\rho N g B}{2c} N_\gamma + N_c \tag{1}$$

where $\rho$: bulk density of the soil, $Ng$: gravitational acceleration level, $B$: footing breadth. $N_c$ and $N_\gamma$ represent the bearing

capacity factors with respect to cohesion and self weight of soil, respectively.

The calculation results of $q_u/c$ for lunar soil stimulant in $D_r$ = 60 % ($\phi'$ = 41.6 deg) obtained from the proposed upper bound analysis are as shown in Figure 9. The figure shows that the ultimate bearing capacity and $N_\gamma$ (slope of the lines) also decreases as $\beta$ increases. This trend accommodates the experimental results that the bearing capacity becomes less dependent on gravity when the passive failure zone dose not appear due to the high compressibility.

Now, the experimental relationships shown in Figure 4 are non-dimensionalized in terms of $\rho NgB/2c$ and $q_u/c$ to rearrange as Figure 9. From this arrangement, $N_\gamma$ and $N_c$ can be revealed through linear approximations of the experimental data. Since $q_u/c$ becomes more susceptible to gravity as the slope of the linear relationship becomes greater, it can be said that the magnitude of $N_\gamma$ represents the sensitivity of gravity against the bearing capacity. The magnitude of $N_\gamma$ for the lunar soil simulant is small compared to that of Toyoura sand, suggesting that the lunar soil simulant is less dependent on gravity than Toyoura sand.

Figure 10 shows the relationships between the internal friction angles and the bearing capacity factors obtained from the upper bound calculations. In addition to the theoretical relationships, experimental values of $N_\gamma$ and $N_c$ are plotted on the charts with respect to each internal friction angle. It can be seen from this figure that experimental value of $N_\gamma$ for lunar soil stimulant is found in the vicinity of $\beta$ = 40 to 45°. This means that the proposed upper bound calculation when $\beta$ = 40 to 45° allows us to take into an account the simulant's dependence on gravity and to predict the ultimate bearing capacity on the lunar soil simulant.

It can be said that the proposed upper bound analysis is interesting in that the soil compressibility (material condition) and the gravity dependence (environmental condition) can be rationally associated to one another. Although a method of estimating $\beta$ as part of the calculation procedure has not yet been proposed, it may become possible to correlate $\beta$ with a soil compressibility parameter since it determines the domain of the failure region.

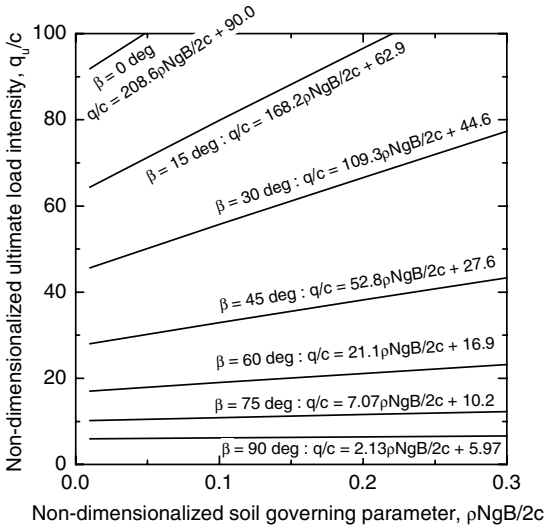


Figure 8. Calculated relationship between ρNgB/2c and $q_u/c$

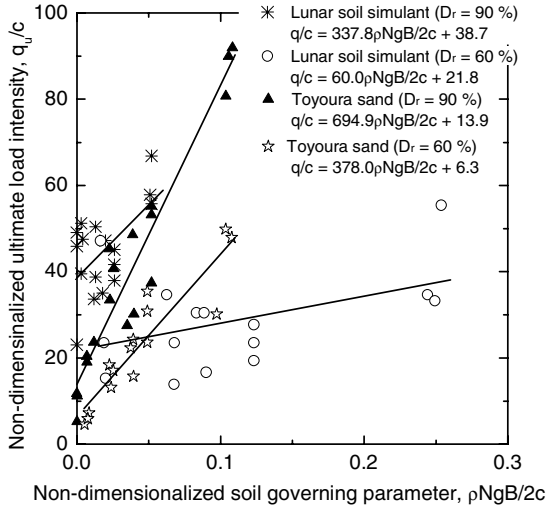


Figure 9. Experimental relationship between ρNgB/2c and $q_u/c$

## 7 CONCLUSIONS

A series of model loading tests on a simulated lunar soil and Toyoura sand were conducted on an aircraft that flew in parabolic paths to generate partial gravity fields. As a result of the model tests, it became clear that bearing characteristics, including the coefficient of subgrade reaction and ultimate bearing capacity, of the lunar soil simulant in a low gravity environment is hardly influenced by the gravity levels, while Toyoura sand exhibits a high dependence on gravity. From the observation of the failure mechanisms, it was found that the gravity dependence seems to correlate with soil compressibility. To rationally explain the dependence of ultimate bearing capacity on gravity, theoretical evaluations were attempted in the framework of the upper bound method. The proposed calculation method not only makes it possible to quantitatively correlate the failure mode with dependence on gravity, but also may allow us to predict the ultimate bearing capacity in the lunar surface environment.

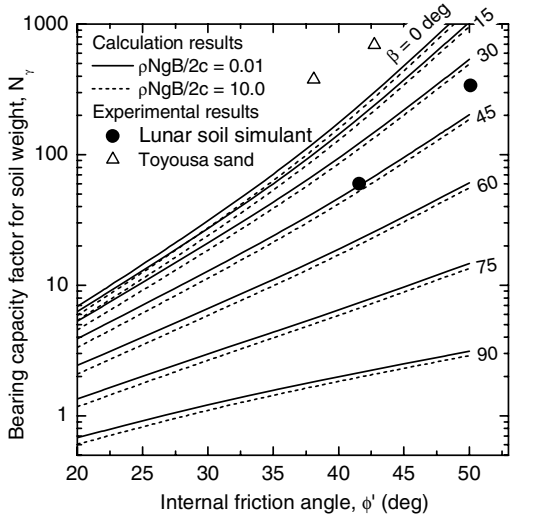


Figure 10. Effect of β on bearing capacity factor

## REFFERENCES

Carrier, W. D. III, Mitchell, J. K., and Mahmood, A. 1973. The Nature of Lunar Soil, *Journal of Soil Mechanics and Foundations Division,* ASCE*s*, 99 (SM10), 813-832.

Carrier, W. D. III, Olhoeft, G., and Mendell, W. W. 1991. Chapter 9; Physical properties of lunar surface, *Lunar Sourcebook*, Cambridge University press, 475-567.

Kanamori, H., Udagawa, S., Yoshida, T., Matsumoto, S., and Takagi, K. 1998. Properties of lunar soil simulant manufactured in Japan, *Proceedings of the 6th International Conference on Engineering, Construction and Operations in Space*, ASCE, 462-468.